Journal of Physics:
Condensed Matter

PAPER • **OPEN ACCESS**

Dynamics of a single anisotropic particle under various resetting protocols

To cite this article: Subhasish Chaki *et al* 2025 *J. Phys.: Condens. Matter* **37** 115101

OPEN ACCESS
IOP Publishing
Journal of Physics: Condensed Matter
J. Phys.: Condens. Matter **37** (2025) 115101 (14pp)
https://doi.org/10.1088/1361-648X/ada336

Dynamics of a single anisotropic particle under various resetting protocols

Subhasish Chaki*, Kristian Stølevik Olsen and Hartmut Löwen

Institut für Theoretische Physik II—Weiche Materie, Heinrich-Heine-Universität Düsseldorf, D-40225 Düsseldorf, Germany

E-mail: Subhasish.Chaki@hhu.de

Received 1 July 2024, revised 2 December 2024
Accepted for publication 24 December 2024
Published 10 January 2025

Abstract

We study analytically the dynamics of an anisotropic particle subjected to different stochastic resetting schemes in two dimensions. The Brownian motion of shape-asymmetric particles in two dimensions results in anisotropic diffusion at short times, while the late-time transport is isotropic due to rotational diffusion. We show that the presence of orientational resetting promotes the anisotropy to late times. When the spatial and orientational degrees of freedom are reset, we find that a non-trivial spatial probability distribution emerges in the steady state that is determined by the initial orientation, particle asymmetry and the resetting rate. When only spatial degrees of freedom are reset while the orientational degree of freedom is allowed to evolve freely, the steady state is independent of the particle asymmetry. When only particle orientation is reset, the late-time probability density is given by a Gaussian with an effective diffusion tensor, including off-diagonal terms, determined by the resetting rate. Generally, the coupling between the translational and rotational degrees of freedom, when combined with stochastic resetting, gives rise to unique behavior at late times not present in the case of symmetric particles. Considering recent developments in experimental implementations of resetting, our results can be useful for the control of asymmetric colloids, for example in self-assembly processes.

Keywords: stochastic resetting, asymmetric colloid, Brownian motion

1. Introduction

A wide variety of processes in physics, chemistry, and biology are comprised of diffusing particles that are highly anisotropic in shape. Prominent examples include rod-like bacteria or viruses [1–4], nematic macromolecules [5, 6], and shape-asymmetric colloids [7–12]. There are several recent research avenues in soft condensed matter, where asymmetric colloidal micro- and nano-particles play a prominent role. In colloidal self-assembly, control of shape-asymmetric particles is crucial for the assembly of materials with novel functions and properties [13–16]. In nanomedicine, how to externally control the dynamics of an asymmetric colloid moving inside the human body is a central question [17].

The diffusive motion of shape-asymmetric objects is a topic with a long history, dating back to the work of Perrin almost a century ago [18–20]. The translational motion of these anisotropic particles can be quite different from those of

* Author to whom any correspondence should be addressed.

spherical particles. When left to diffusive, the anisotropic particles show a crossover from short-time anisotropic diffusion, due to the coupling of rotational and translational motion, to effective isotropic diffusion at late times [21]. The crossover between these regimes depends on the timescale set by the rotational diffusion coefficient, which determines the directional memory along the particle's long axis. Furthermore, the transient behavior of an anisotropic particle is longer-lived in two dimensions when compared to the three-dimensional case. This suggests that the transient behavior may modulate the reaction rate of diffusion-limited reactions in intracellular membranes, where reaction time is frequently of the order of microseconds and the environment is dimensionally restricted [22, 23]. Experimental methods are also available for synthesizing and characterizing the dynamics of ellipsoidal colloids [21]. Experimentally, it has been shown that the transition from anisotropic to isotropic diffusion in two dimensions occurs over a period of a few seconds for a free micrometer-sized ellipsoidal particle [24].

The Brownian motion of an anisotropic particle has been studied in many situations over the years, including dynamics in confinement and external potentials [24, 25], first passage analysis [26, 27], active matter [28–30] and stochastic thermodynamics [31]. So far, to the best of our knowledge, there has been little or no work on anisotropic particles subjected to *stochastic resetting*. Stochastic resetting is a process whereby a system's state is brought back to its initial condition at a constant rate [32–34]. A wide range of intriguing phenomena results from this simple rule of intermittent interruption, for example, anomalous relaxation properties [35, 36] and non-trivial steady states resulting from the confining effect of resetting [37, 38]. Over recent years, a myriad of aspects has been investigated, including target search processes under resets [39–55], stochastic thermodynamics [56–65], and active matter [66–71]. Recently, the effects of resetting in systems with multiple coupled degrees of freedom have been studied. In particular, the case where an observed degree of freedom experiences indirect effects of resets due to a coupling to a resetting variable has been investigated [72, 73].

In the majority of past studies, resetting is applied to symmetric or point-like particles. Here, we extend past studies by studying the effect of various resetting schemes applied to a shape-asymmetric Brownian particle. In particular, we consider the case of a Brownian anisotropic particle, where a rotational-translational coupling is present which separates the dynamics from the symmetric counterpart. We study the dynamics of a Brownian anisotropic particle under various resetting schemes, all of which may be implemented experimentally. Resetting of the translational degrees of freedom can be achieved by optical tweezers [40, 45, 65, 74], while resetting of the particle's orientation can be performed using techniques developed for magnetic anisotropic colloid assembly [75]. We seek to understand the dynamical consequences of the combined effect of particle asymmetry and resetting in two dimensions, which can be characterized by moments and marginal distributions, available, for example, in colloidal experiments using particle tracking.

This paper is structured as follows. Section 2 introduced the necessary background theory, including the Brownian motion of anisotropic particles in two dimensions, as well as the renewal approach to stochastic resetting when multiple degrees of freedom is present. We then proceed to investigate the dynamical and stationary properties under various resetting schemes, namely complete resetting of all degrees of freedom, translational resetting, and orientational resetting in sections 3–5 respectively. Section 6 offer a concluding discussion.

2. General theory

2.1. Diffusion of an anisotropic particle

Here we consider the dynamics of an anisotropic free Brownian particle in two dimensions with mobilities $\Gamma_{||}$ and $\Gamma_{\perp}$ along the longer and the shorter axes of the particle, as shown in figure 1(a) respectively. Additionally, the motion of the particle is subjected to rotational diffusion, characterized by the mobility Γ_θ. The translational and rotational diffusivities are defined through Einstein-Smoluchowski relations $D_{||} = k_B T \Gamma_{||}$ and $D_{\perp} = k_B T \Gamma_{\perp}$, and $D_\theta = k_B T \Gamma_\theta$, where T is the temperature of the bath. The particle at any given time t can be described by the position vector $\vec{r}(t)$ of its center of mass, which can be decomposed as $(\delta\tilde{x}, \delta\tilde{y})$ in the body frame and $(\delta x, \delta y)$ in the laboratory frame. The angle between the lab and body frames is denoted as $\theta(t)$, which evolves diffusively as

$$\frac{\partial\theta}{\partial t} = \sqrt{2k_B T\Gamma_\theta}\tilde{\eta}_\theta(t). \tag{1}$$

The translational motions of the anisotropic particle are decoupled in the body frame, and are described by the Langevin equations,

$$\frac{\partial\tilde{x}}{\partial t} = \sqrt{2k_B T\Gamma_{\parallel}}\tilde{\eta}_x(t); \ \frac{\partial\tilde{y}}{\partial t} = \sqrt{2k_B T\Gamma_{\perp}}\tilde{\eta}_y(t). \tag{2}$$

Without any loss of generality, we assume that the longer and the shorter axes of the particle are along the $\tilde{x}$ and $\tilde{y}$ directions of the body frame respectively. The translational and rotational noise terms $\tilde{\eta}_\theta(t)$, $\tilde{\eta}_x(t)$ and $\tilde{\eta}_y(t)$ in equations (1) and (2) are assumed to be Gaussian and characterized by the following mean and variances

$$\langle\tilde{\eta}_i(t)\rangle = 0, \text{ and } \langle\tilde{\eta}_i(t)\tilde{\eta}_j(t')\rangle = \delta_{ij}\delta(t-t') \tag{3}$$

The displacements in the lab and the body frames are related by the following equations,

$$\begin{aligned}\delta x &= \cos\theta\delta\tilde{x} - \sin\theta\delta\tilde{y},\\ \delta y &= \cos\theta\delta\tilde{y} + \sin\theta\delta\tilde{x}.\end{aligned} \tag{4}$$

Dividing the equation (4) by δt, taking the limit $\delta t \to 0$, and substituting the translational velocities in the body frame from equation (2), we get the equations of motion in the lab frame as follows

$$\frac{\partial x}{\partial t} = \xi_x(t); \ \frac{\partial y}{\partial t} = \xi_y(t) \tag{5}$$

The random variables ξ_i have zero mean and the correlations at fixed $\theta(t)$ are given by

$$\langle \xi_i(t)\,\xi_j(t')\rangle = 2k_B T \Gamma_{ij}[\theta(t)]\,\delta(t-t'), \tag{6}$$

where $\Gamma_{ij}[\theta(t)] = \frac{\bar{\Gamma}}{2} + \frac{\Delta\Gamma}{2}\begin{bmatrix} \cos 2\theta(t) & \sin 2\theta(t) \\ \sin 2\theta(t) & -\cos 2\theta(t) \end{bmatrix}$ with $\bar{\Gamma} = \frac{\Gamma_{||}+\Gamma_{\perp}}{2}$ and $\Delta\Gamma = \frac{\Gamma_{||}-\Gamma_{\perp}}{2}$.
Integrating equation (5) with respect to time for x direction, one obtains

$$x(t) = \int_0^t dt' \xi_x(t') + x_0. \tag{7}$$

The rotational degree of freedom evolves on the unit circle following an ordinary Brownian that is independent of the translational degrees of freedom. Hence, the second moment of the particle, conditional on an initial orientation angle θ_0, can be explicitly calculated from equation (7) as

$$\begin{aligned}\langle x^2(t)\,|\theta_0\rangle &= \int_0^t dt' \int_0^t dt'' \langle \xi_i(t')\,\xi_i(t'')\rangle \\ &= 2k_B T \int_0^t dt' \int_0^t dt'' \langle \Gamma_{ij}[\theta(t')]\rangle_{\eta_\theta} \delta(t'-t'') \\ &= 2k_B T \int_0^t dt' \left[\bar{\Gamma} + \frac{\Delta\Gamma}{2}\langle \cos\theta(t')\,|\theta_0\rangle\right] \\ &= 2k_B T \left[\bar{\Gamma} t + \frac{\Delta\Gamma}{2}\cos 2\theta_0 \left(\frac{1-e^{-4D_\theta t}}{4D_\theta}\right)\right] \end{aligned} \tag{8}$$

Here, and throughout, we assume the particle is initially at the origin $x_0 = y_0 = 0$. Above, we used the following identity

$$\begin{aligned}\langle \cos 2\theta(t)\,|\theta_0\rangle &= Re\langle e^{i2\theta}|\theta_0\rangle = Re\left[\int d\theta e^{i2\theta} \frac{e^{-\frac{(\theta-\theta_0)^2}{4D_\theta t}}}{\sqrt{4\pi D_\theta t}}\right] \\ &= \cos(2\theta_0)\, e^{-4D_\theta t} \end{aligned} \tag{9}$$

Similarly, one can explicitly calculate the second moment for $y(t)$ direction

$$\langle y^2(t)\,|\theta_0\rangle = 2k_B T \left[\bar{\Gamma} t - \frac{\Delta\Gamma}{2}\cos 2\theta_0 \left(\frac{1-e^{-4D_\theta t}}{4D_\theta}\right)\right] \tag{10}$$

The first term in equations (8) and (10) is attributed to the diffusion of the center-of-mass and the second term results from the displacement of the particle due to the orientational fluctuations. At late times much larger than the rotational timescale $t \gg D_\theta^{-1}$, the diffusion is isotropic with $\langle x^2(t)\rangle = \langle y^2(t)\rangle = 2k_B T \bar{\Gamma} t$. At short timescales, however, we have the first-order expansions

$$\langle x^2(t)\,|\theta_0\rangle = 2k_B T \left(\bar{\Gamma} + \frac{\Delta\Gamma}{2}\cos(2\theta_0)\right) t + \mathcal{O}(t^2) \tag{11}$$

$$\langle y^2(t)\,|\theta_0\rangle = 2k_B T \left(\bar{\Gamma} - \frac{\Delta\Gamma}{2}\cos(2\theta_0)\right) t + \mathcal{O}(t^2) \tag{12}$$

where we see that the shape asymmetry gives rise to anisotropic diffusion at early times, depending on the particle's initial orientation θ_0. It is interesting to compare the mean squared displacements along the x and y directions. The ratio of the variances is given by $K = \frac{\langle x^2(t)|\theta_0\rangle}{\langle y^2(t)|\theta_0\rangle} = \frac{\left(\bar{\Gamma}+\frac{\Delta\Gamma}{2}\cos(2\theta_0)\right)}{\left(\bar{\Gamma}-\frac{\Delta\Gamma}{2}\cos(2\theta_0)\right)}$.
The anisotropy in diffusion also generates non-zero cross-correlation between x and y through their mutual coupling to the orientation,

$$\langle x(t)\,y(t)\,|\theta_0\rangle = 2k_B T \left[\frac{\Delta\Gamma}{2}\sin 2\theta_0 \left(\frac{1-e^{-4D_\theta t}}{4D_\theta}\right)\right]. \tag{13}$$

It is evident that the correlation between x and y in equation (13) becomes constant at $t \to \infty$ due to the decorrelation between θ_0 and $\theta(t)$ after a timescale proportional to D_θ^{-1}.

2.2. Renewal approach to resetting

The anisotropic particle in two dimensions can be described by its center-of-mass positions, (x, y) as well as an orientation angle θ. We collect these three degrees of freedom into a single phase space variable $X \equiv (x, y, \theta)$. Upon stochastic resetting, we must prescribe a rule for how all phase space variables are reset. In general, we assume that upon a reset event the phase space point $X(t)$ resets to

$$X(t) \longrightarrow X_R(X_0, X(t)) \tag{14}$$

where the resetting location $X_R(X_0, X(t))$ can be a mix of the coordinates $X(t)$ before the reset and the initial coordinates X_0 depending on the type of resetting considered. For Poissonian resets, i.e. the waiting time between resets follows an exponential distribution with rate r, the full phase space propagator $P_r(X, t|X_0)$ can be expressed in terms of a renewal equation

$$\begin{aligned}P_r(X, t|X0) &= e^{-rt} P_0(X, t|X_0) + r\int_0^t d\tau e^{-r\tau} \\ &\times \int dX' P_r(X', t-\tau|X_0)\, P_0(X, \tau|X_R(X_0, X')). \end{aligned} \tag{15}$$

The equation (15) is based on the renewal property of resetting processes, with simpler single-variable versions having been widely utilized in previous studies [34]. In this work, we employ a renewal equation tailored for multivariable systems, where resetting is applied to only a subset of the states. In the above, $P_0(X, t|X_0)$ is the propagator of the underlying system

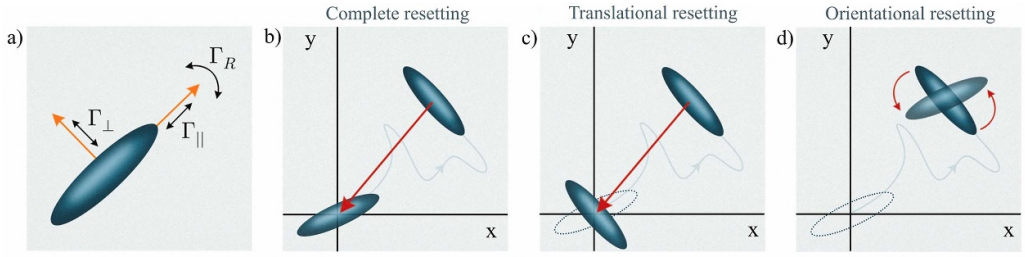

Figure 1. (a) Anisotropic particle with three mobilities; parallel to body axis $\Gamma_{||}$, perpendicular to the body axis $\Gamma_\perp$, and a rotational motility Γ_R. (b) Under complete resetting, all degrees of freedom are reset to their initial conditions. (c) For translational resets, only the particle's center-of-mass position is reset. (d) Under orientational resetting, the particle orientation angle is reset, while the center-of-mass positions remain unchanged.

in the absence of resetting. The first term in equation (15) corresponds to trajectories where no resets have occurred up to time t, which happens with probability e^{-rt}. The second term takes into account trajectories where one or more resetting events takes place. The particle propagates up to the time of the last resetting, $t-\tau$, with the propagator $P_r(X',t-\tau|X_0)$, residing in a random state X' at this instance. After the subsequent reset $X' \to X_R(X_0,X')$ the particle propagates from this point to the final state without further resets, with propagator $P_0(X,\tau|X_R(X_0,X'))$.

While an exact solution of the propagator in equation (15) is often hard to find, it provides a powerful tool to calculate the expected value of an observable $\mathcal{O}(X)$ [71]. Multiplying both sides of equation (15) with $\mathcal{O}(X)$ and integrating over all possible X, we find

$$\langle \mathcal{O}(X,t)|X_0\rangle_r = \mathrm{e}^{-rt}\langle \mathcal{O}(X,t)|X_0\rangle_0 + r\int_0^t \mathrm{d}\tau \mathrm{e}^{-r\tau}\int \mathrm{d}X' P_r \times (X',t-\tau|X_0)\,\langle \mathcal{O}(X,\tau)|X_R(X_0,X')\rangle_0 \tag{16}$$

In the following, we use this approach to calculate observables under various resetting protocols for the anisotropic particle.

Stochastic resetting can be approached through two equivalent frameworks: the renewal equation approach, which we utilize here, and the Fokker–Planck equation approach. To validate the consistency of these approaches, we derive the last renewal equation for partial resetting directly from the Fokker–Planck formulation. The detailed derivation is provided in the appendix. We consider the following resetting protocols by changing the functional form of the resetting point in phase space $X_R(X_0,X(t))$:

i) **Complete resetting:** all phase space variables are reset to their initial values $X_R(X_0,X'(t)) = X_0$, shown in the schematic in figure 1(b).
ii) **Translational resetting:** only the spatial coordinates are reset, i.e. $X_R(X_0,X'(t)) = (x_0,y_0,\theta'(t))$, shown in the schematic in figure 1(c).
iii) **Orientational resetting:** only the orientation is reset $X_R(X_0,X'(t)) = (x'(t),y'(t),\theta_0)$, shown in the schematic in figure 1(d).

In the following, we consider these cases separately. In particular, we are interested in the reduced dynamics of one of the spatial coordinates, for which reduced renewal equations are derived in each case.

3. Complete resetting

For complete resetting, the propagator $P_r(X,t|X_0)$ in the presence of Poissonian resetting can be written through the last renewal equation

$$P_r(X,t|X_0) = \mathrm{e}^{-rt}P_0(X,t|X_0) + r\int_0^t \mathrm{d}\tau \mathrm{e}^{-r\tau} \times \int \mathrm{d}X_0 P(X_0)\,P_0(X,\tau|X_0)\,. \tag{17}$$

Here we have assumed that the initial condition X_0 is drawn from a distribution $P(X_0)$. The last renewal equation can predict the steady state as

$$P_{\mathrm{st}}(X,t|X_0) = r\int_0^\infty d\tau e^{-r\tau}\int dX_0 P(X_0)\,P(X,\tau|X_0) = r\int dX_0 P(X_0)\,\tilde{P}_0(X,r|X_0) \tag{18}$$

Here $\tilde{P}_0(X,r|X_0)$ is the Laplace transform of $P_0(X,\tau|X_0)$.

Using the method outlined above to derive equation (16), the renewal equation for the moments can similarly be obtained from the last renewal equation, equation (17)

$$\langle X^n(t)\rangle_r = \mathrm{e}^{-rt}\langle X^n(t)\rangle_0 + r\int_0^t \mathrm{d}\tau \mathrm{e}^{-r\tau}\int \mathrm{d}X_0 P(X_0)\,\langle X^n(\tau)\rangle_0. \tag{19}$$

For our case, X represents three dynamical variables (x,y,θ). For a fixed initial state $X_0 = (0,0,\theta_0)$, we have

$$P_r(x,y,\theta,t|0,0,\theta_0) = \mathrm{e}^{-rt}P_0(x,y,\theta,t|0,0,\theta_0) + r\int_0^t \mathrm{d}\tau \mathrm{e}^{-r\tau}P_0(x,y,\theta,\tau|0,0,\theta_0)\,. \tag{20}$$

The effect of resetting on the variable x can be obtained by integrating over y and θ in the above renewal equation:

$$P_r(x,t|0,\theta_0) = \mathrm{e}^{-rt}P_0(x,t|0,\theta_0) + r\int_0^t \mathrm{d}\tau \mathrm{e}^{-r\tau}P_0(x,\tau|0,\theta_0). \tag{21}$$

The corresponding moments for x in that case would be

$$\langle x^n(t)|\theta_0\rangle_r = \mathrm{e}^{-rt}\langle x^n(t)|\theta_0\rangle_0 + r\int_0^t \mathrm{d}\tau \mathrm{e}^{-r\tau}\langle x^n(\tau)\rangle_{\theta_0}. \tag{22}$$

Next, we calculate the second moment of x using equation (8) and $n=2$ in the equation (22),

$$\langle x^2(t)|\theta_0\rangle_r = \frac{2k_BT\bar{\Gamma}}{r}\left(1-\mathrm{e}^{-rt}\right) + \frac{k_BT\Delta\Gamma\cos 2\theta_0}{(r+4D_\theta)}\left(1-\mathrm{e}^{-(r+4D_\theta)t}\right). \tag{23}$$

Similarly, one can also calculate $\langle y^2(t)|\theta_0\rangle_r$ and the cross-correlation $\langle x(t)y(t)|\theta_0\rangle_r$ in the presence of resetting. We find

$$\langle y^2(t)|\theta_0\rangle_r = \frac{2k_BT\bar{\Gamma}}{r}\left(1-\mathrm{e}^{-rt}\right) - \frac{k_BT\Delta\Gamma\cos 2\theta_0}{(r+4D_\theta)}\left(1-\mathrm{e}^{-(r+4D_\theta)t}\right) \tag{24}$$

$$\langle x(t)y(t)|\theta_0\rangle_r = \frac{k_BT\Delta\Gamma\sin 2\theta_0}{(r+4D_\theta)}\left(1-\mathrm{e}^{-(r+4D_\theta)t}\right). \tag{25}$$

To gain further insights into the dynamics, we consider the dynamical exponents $\zeta_x(t) = \frac{\mathrm{d}\left[\log\langle x^2(t)\rangle\right]}{\mathrm{d}[\log t]}$ and $\zeta_y(t) = \frac{\mathrm{d}\left[\log\langle y^2(t)\rangle\right]}{\mathrm{d}[\log t]}$ for both x and y directions respectively. These are plotted in figure (2). In figure (2), we chose the particle initially oriented along the x direction. Without resetting, the exponent $\zeta(t)$ clearly exhibits three distinct regimes—short time diffusive regime ($\zeta_{x,y}(t)\approx 1$) for both the x and y directions, intermediate superdiffusion ($\zeta_y(t)>1$) for y direction and subdiffusion ($\zeta_x(t)<1$) for x direction and long time diffusive motion ($\zeta_{x,y}(t)\approx 1$) for both the x and y directions. A transition to confined motion ($\zeta_{x,y}(t)\approx 0$) occurs in the presence of resetting. At a very short times, $t \ll \min(r^{-1}, D_\theta^{-1})$, the particle moves diffusively in each direction with different mobilities $\Gamma_{||}$ and $\Gamma_\perp$ for $\theta_0 = 0$ as shown in equations (12), and the motion is not yet affected by resetting. After the characteristic timescale set by rotational diffusion, the particle performs diffusive motion with an effective diffusion constant $\bar{D}$ due to the decorrelation in the orientational degrees of freedom. Since the mobility in the x and y directions are larger and smaller than $\bar{D}$ respectively, the motion in these directions must be decelerated or accelerated to reach the isotropic diffusivity $\bar{D}$ in the long time limit. In the presence of resetting, a transition to confinement ($\zeta_{x,y}\approx 0$) occurs at a typical time r^{-1}, potentially interrupting the other dynamical regimes.

Since resetting bring the particle orientation back to its initial angle, the anisotropy found in the short-time expansions equation (12) is partially promoted to late times. To see this, we consider as a measure for the late-time anisotropy the ratio of the mean squared displacements in the x and y directions. In the absence of resetting, the steady-state second moment in the presence of resetting for a spherical Brownian particle with diffusivity $\bar{D}$ is $\frac{2\bar{D}}{r}$ along both the x and y directions. However, the steady-state second moments in the presence of resetting for the anisotropic particle are modified and become larger or smaller than $\frac{2\bar{D}}{r}$ in the x and y directions. Indeed, at late times $\langle x^2|\theta_0\rangle = \frac{2\bar{D}}{r} + \frac{k_BT\Delta\Gamma\cos 2\theta_0}{(r+4D_\theta)}$ and $\langle y^2|\theta_0\rangle = \frac{2\bar{D}}{r} - \frac{k_BT\Delta\Gamma\cos 2\theta_0}{(r+4D_\theta)}$. The ratio of the variances is given by

$$K_r = \frac{\langle x^2(t)|\theta_0\rangle_r}{\langle y^2(t)|\theta_0\rangle_r} = \frac{\frac{2\bar{D}}{r} + \frac{k_BT\Delta\Gamma\cos 2\theta_0}{(r+4D_\theta)}}{\frac{2\bar{D}}{r} - \frac{k_BT\Delta\Gamma\cos 2\theta_0}{(r+4D_\theta)}}. \tag{26}$$

In the case of a spherical particle ($\Delta\Gamma = 0$), one obtains $K_r = 1$ independent of the stochastic resetting. The motion is not isotropic for $\Delta\Gamma \neq 0$ under the resetting of all the variables, and the degree of anisotropy increases with r and eventually saturates, as shown in figure (3). The timescale of the cross-correlation between x and y directions is renormalized in the presence of resetting, but the form remains invariant (see equations (13) and (25)).

3.1. Perturbative steady state for near-symmetric particles

While we can derive exact expressions for the lower-order moments as discussed above, we would also like to gain insights into the overall shape of the non-equilibrium steady state under resetting. To achieve this, we consider for simplicity a perturbative approach where we calculate the propagator in the absence of resetting, and then use the renewal approach to resetting in order to find the steady state.

In the absence of resetting, the dynamics can be described by the Smoluchowski–Perrin equation

$$\partial_t P_0(X,t|X_0) = D_\theta\partial_\theta^2 P_0(X,t|X_0) + \nabla\cdot[\mathbb{D}\cdot\nabla]P_0(X,t|X_0), \tag{27}$$

where $\mathbb{D}$ is the diffusion tensor $\mathbb{D}_{ij} = k_BT\Gamma_{ij} = D_{||}n_in_j + D_\perp(\delta_{ij}-n_in_j)$with $\boldsymbol{n} = (\cos\theta, \sin\theta)$ the unit vector pointing along the particle's major axis.

Performing a Fourier transform to the equation (27), we find

$$\partial_t\hat{P}_0(\boldsymbol{k},\theta,t|\theta_0) = D_\theta\partial_\theta^2\hat{P}_0(\boldsymbol{k},\theta,t|\theta_0) + \boldsymbol{k}\cdot[\mathbb{D}\cdot\boldsymbol{k}]\hat{P}_0(\boldsymbol{k},\theta,t|\theta_0). \tag{28}$$

where $\hat{P}_0(\boldsymbol{k},\theta,t|\theta_0) \equiv \int \mathrm{d}\boldsymbol{x}\mathrm{e}^{-i\boldsymbol{k}\cdot\boldsymbol{x}}P_0(\boldsymbol{x},\theta,t|\theta_0)$.

For simplicity, we here consider the steady state in the x-direction. Hence, we consider a wave vector $\boldsymbol{k} = k\boldsymbol{e}_x$, with $\boldsymbol{e}_x$

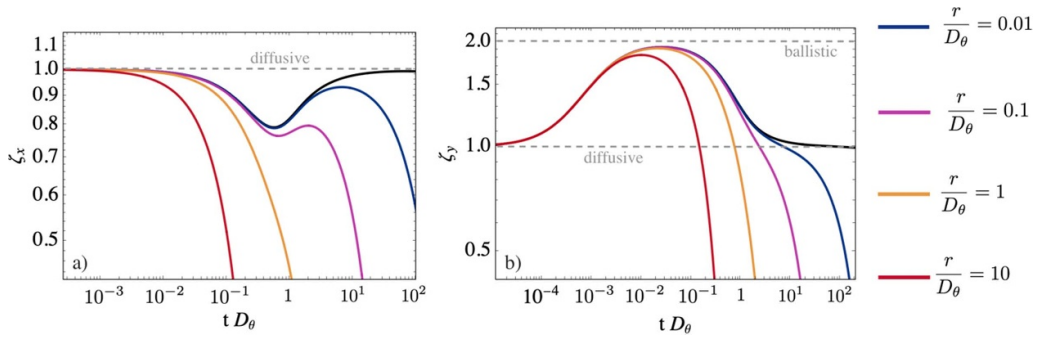

Figure 2. Dynamical exponents $\zeta_x(t)$ and $\zeta_y(t)$ for the mean squared displacement in the x and y direction for various values of resetting rate. The black line shows the exponents without resetting. Parameters are set to $\bar{\Gamma} = 1.0$, $\Delta\Gamma = 0.001$, with initial orientation $\theta_0 = 0$.

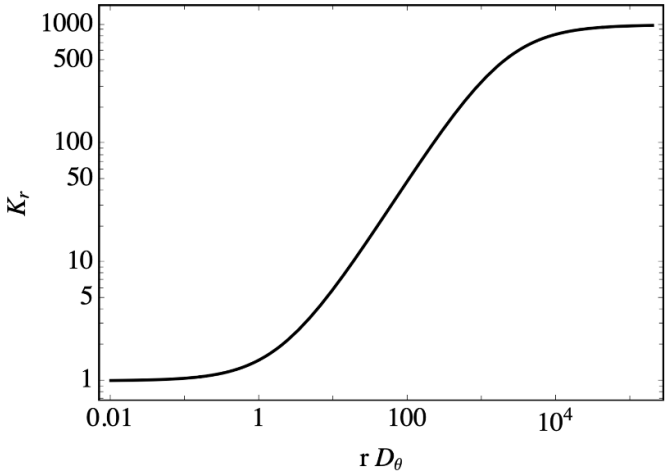

Figure 3. Ratio of variances K_r as a function of resetting rate. The anisotropy grows with resetting rate, and saturates in the $r \to \infty$ limit.

the unit vector in the x-direction. The marginal distribution in the x direction for equation (28) satisfies [76]

$$\partial_t P_0(k,\theta,t|\theta_0) = \left[D_\theta \partial_\theta^2 - k^2\left(\bar{D} + \frac{\Delta D}{2}\cos(2\theta)\right)\right] \times P_0(k,\theta,t|\theta_0). \tag{29}$$

A natural interpretation of the equation (29) is that the effective diffusivity in the x-direction $\bar{D} + \frac{\Delta D}{2}\cos(2\theta)$ depends on the orientation of the particle. To find an analytical solution of equation (29) that provides some insight into the shape of the steady state under resetting, we consider a perturbative approach, where we expand $P_0(k,\theta,t|\theta_0)$ in power of the dimensionless asymmetry parameter $\varepsilon \equiv \Delta D/\bar{D}$. We simplify the Fourier transformed marginal Smoluchowski-Perrin equation (29) as

$$\partial_t P_0(k,\theta,t|\theta_0) = D_\theta \partial_\theta^2 \hat{P}_0(k,\theta,t|\theta_0) - k^2\bar{D}\hat{P}_0 - \varepsilon\, k^2\bar{D}\frac{\cos(2\theta)}{2}\hat{P}_0(k,\theta,t|\theta_0). \tag{30}$$

Next, we expand $P_0(k,\theta,t|\theta_0)$ in powers of the asymmetry parameter ε as

$$P_0(k,\theta,t|\theta_0) = \sum_{n=0}^{\infty} p_n(k,\theta,t|\theta_0)\,\varepsilon^n. \tag{31}$$

where $p_n(k,\theta,t|\theta_0)$ is the coefficient function of the power series. Inserting this ansatz (equation (31)) into the Fourier transformed Smoluchowski–Perrin equation (30) gives the coupled equations

$$\partial_t p_0(k,\theta,t|\theta_0) = D_\theta \partial_\theta^2 p_0(k,\theta,t) - k^2\bar{D}p_0(k,\theta,t|\theta_0) \text{ for } n = 0, \tag{32}$$

$$\partial_t p_n(k,\theta,t|\theta_0) = \left[D_\theta\partial_\theta^2 - k^2\bar{D}\right]p_n(k,\theta,t|\theta_0) - \frac{k^2\bar{D}\cos(2\theta)}{2}p_{n-1}(k,\theta,t|\theta_0) \text{ for } n \geqslant 1. \tag{33}$$

First, we note that $p_0(k,\theta,t)$ is nothing but the Gaussian solution of a symmetric colloid. As we are interested in the spatial steady state to first order, we integrate over the angular variable for $n = 0, 1$ in the above equations (32) and (33), leading to

$$\partial_t p_0(k,t) = -k^2\bar{D}p_0(k,t), \tag{34}$$

$$\partial_t p_1(k,t|\theta_0) = -k^2\bar{D}p_1(k,t|\theta_0) - k^2\bar{D}p_0(k,t)\int \mathrm{d}\theta \frac{\cos(2\theta)}{2}\frac{\exp\left(-\frac{(\theta-\theta_0)^2}{4D_\theta t}\right)}{\sqrt{4\pi D_\theta t}} \tag{35}$$

where we used the fact that the angular displacement is a Gaussian random variable. Here the zeroth order solution of equation (34) reads

$$p_0(k,t) = \mathrm{e}^{-\bar{D}k^2 t}. \tag{36}$$

The integration in equation (35) for the first order correction can be carried out exactly by using equation (9), yielding

$$\partial_t p_1(k,t|\theta_0) = -k^2\bar{D}p_1(k,t|\theta_0) - k^2\bar{D}\cos(2\theta_0)\,p_0(k,t)\,\frac{e^{-4D_\theta t}}{2}. \tag{37}$$

Substituting equations (36) in (37) and performing a Laplace transform for time t results in

$$\hat{\tilde{p}}_1(k,s|\theta_0) = -\frac{k^2\bar{D}\cos(2\theta_0)}{2(s+4D_\theta+\bar{D}k^2)(s+k^2\bar{D})} \tag{38}$$

where $\tilde{\hat{p}}_1(k,s|\theta_0) = \int_0^\infty dt e^{-st}\hat{p}_1(k,t|\theta_0)$. Inverting the Fourier transform of equation (38), we arrive at the first order correction to the propagator in the Laplace domain as

$$\begin{aligned}\tilde{p}_1(x,s|\theta_0) &= \cos(2\theta_0)\,\frac{\alpha(s)}{16D_\theta}e^{-\alpha(s)|x|} \\ &\quad - \cos(2\theta_0)\,\frac{\alpha(s+4D_\theta)}{16D_\theta}e^{-\alpha(s+4D_\theta)|x|}\end{aligned} \tag{39}$$

where we introduced the inverse lengthscale $\alpha(s) \equiv \sqrt{s/\bar{D}}$. Thus, the spatial probability distribution up to the first order correction without resetting in the Laplace domain would be

$$\begin{aligned}\tilde{P}_0(x,s|\theta_0) &= \tilde{p}_0(x,s|\theta_0) + \varepsilon\tilde{p}_1(x,s|\theta_0) \\ &= \frac{\alpha(s)}{2}e^{-\alpha(s)|x|} + \varepsilon\cos(2\theta_0)\,\frac{\alpha(s)}{16D_\theta}e^{-\alpha(s)|x|} \\ &\quad - \varepsilon\cos(2\theta_0)\,\frac{\alpha(s+4D_\theta)}{16D_\theta}e^{-\alpha(s+4D_\theta)|x|}\end{aligned} \tag{40}$$

where $\tilde{p}_0(x,s|\theta_0)$ is obtained from equation (36) by applying Laplace transformation in time and inverse Fourier transformation in space [34]. The term $\tilde{P}_0(x,s|\theta_0)$ represents a normalized probability distribution. Since $\tilde{p}_0(x,s|\theta_0)$ is already a normalized distribution, the normalization condition on $\tilde{P}_0(x,s|\theta_0)$ requires that the integral of the perturbative term, $\tilde{p}_1(x,s|\theta_0)$ over all x, must equal zero due to having both positive and negative values.

We can now easily obtain the steady state under the effect of resetting by using the renewal equation (21), and letting $t \to \infty$ as

$$P_r(x|0,\theta_0) = r\int_0^\infty d\tau e^{-r\tau}P_0(x,\tau|0,\theta_0) = r\tilde{P}_0(x,r|0,\theta_0). \tag{41}$$

Substituting of equation (40) in equation (41) and replacing s by r yields the first order correction of the spatial probability distribution along x direction with resetting as

$$\begin{aligned}P_r(x|\theta_0) &= \frac{\alpha(r)}{2}e^{-\alpha(r)|x|} + \varepsilon\cos(2\theta_0)\left[\frac{r\alpha(r)}{16D_\theta}e^{-\alpha(r)|x|}\right. \\ &\quad \left. - \frac{r\alpha(r+4D_\theta)}{16D_\theta}e^{-\alpha(r+4D_\theta)|x|}\right].\end{aligned} \tag{42}$$

Several things are worth noting. The zeroth order solution of the steady state probability distribution is determined by a single length scale $\alpha(r)$ set by resetting. It shows a peak at $x=0$ in figure 4(a) due to the confining effect of the resetting towards the origin. This peak value increases with increasing the resetting rate r in figure 5(a), as is expected. Once particle asymmetry is introduced, the solution also depends on the length scale set by $\alpha(r+4D_\theta)$, and in addition depends on the initial orientation θ_0. Here, the rotational dynamics enter into the spatial steady state due to the coupling between the translational and rotational degrees of freedom, which persists to late times as discussed above. Figure 4(b) shows that the first order correction to the distribution is negative at $x=0$ for $\theta_0=0$, which is consistent with the enhanced motion along the x direction; hence the steady state widens in this case. When $\theta_0=\pi/2$, the long axis of the anisotropic particle will be along the y axis, resulting in the suppression of the mobility along the x direction relative to the isotropic diffusivity $\bar{D}$. Consequently, the motion in x direction is accelerated at the intermediate time to achieve $\bar{D}$ in the long time limit, as discussed in section 3. This accelerated motion enhances spatial displacement in the x direction, resulting in a positive first-order correction to the spatial distribution at $x=0$. A similar argument applies for $\theta_0=0$, where the first-order correction to the spatial distribution along the x direction becomes negative at $x=0$. The intermediate angles $2\pi/10$ and $7\pi/10$ represent gradual transition of particle orientation and the corresponding changes in mobility along the x direction between the two limiting cases of $\theta_0=0$ and $\theta_0=\pi/2$. The peak value of the first-order correction also increases with the resetting rate r, as seen in figure 5(b). This is consistent with the observation that the degree of anisotropy K_r increases with increasing resetting rate r.

4. Translational resetting

Next, we consider the case where x and y undergo resets while the orientational degree of freedom θ variable does not reset. Following the discussion in section 2.2, we have the renewal equation

$$\begin{aligned}P_r(x,y,\theta,t|0,0,\theta_0) &= e^{-rt}P_0(x,y,\theta,t|0,0,\theta_0) \\ &\quad + r\int_0^t d\tau e^{-r\tau}\int dx'\int dy'\int d\theta' P_r(x',y',\theta',t-\tau|0,0,\theta_0) \\ &\quad \times P_0(x,y,\theta,\tau|0,0,\theta').\end{aligned} \tag{43}$$

The propagator for x for this case can be obtained by integrating the above equation over y, θ, x' and y',

$$\begin{aligned}P_r(x,t|0,\theta_0) &= e^{-rt}P_0(x,t|0,\theta_0) + r\int_0^t d\tau e^{-r\tau} \\ &\quad \times \int d\theta' P_0(\theta',t-\tau|\theta_0)\,P_0(x,\tau|0,\theta').\end{aligned} \tag{44}$$

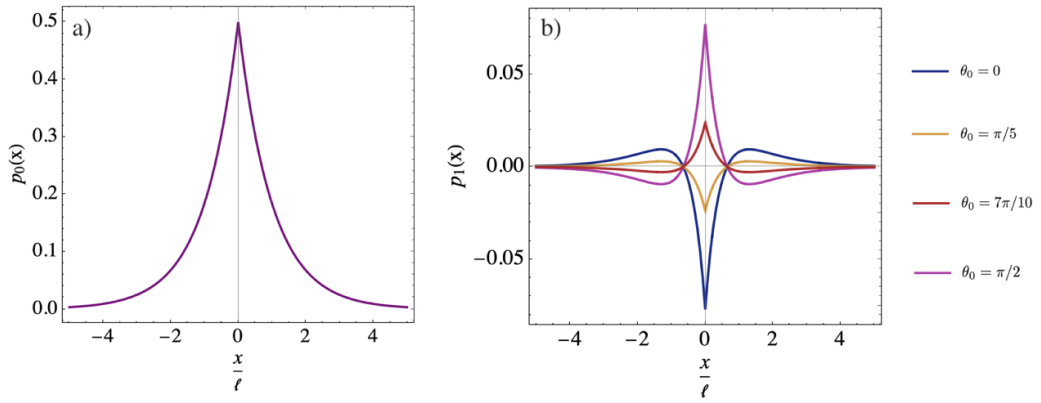

Figure 4. Steady state marginal density under complete resetting. (a) Zeroth order solution corresponding to the standard Laplacian solution for a spherical Brownian particle with diffusivity $\bar{D}$. (b) First order correction to the steady state for a Brownian anisotropic particle for various θ_0. The lengthscale is set by $\ell^2 = 2k_BT\bar{\Gamma}/D_\theta$, and the parameters are set to $D_\theta = \bar{D} = r = 1$.

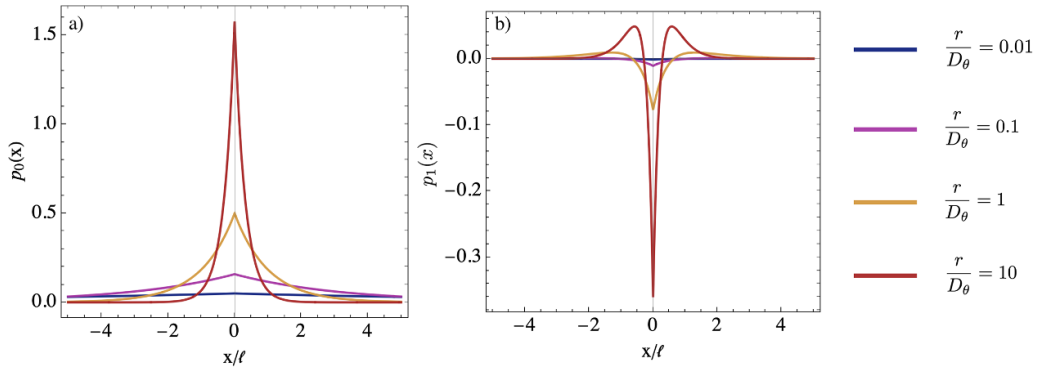

Figure 5. Steady state marginal density under complete resetting. (a) Zeroth order solution corresponding to a spherical Brownian particle at different resetting rates. (b) First order correction to the steady state for a Brownian anisotropic particle for various resetting rates. The lengthscale is set by $\ell^2 = 2k_BT\bar{\Gamma}/D_\theta$, and the parameters are set to $D_\theta = \bar{D} = r = 1$, $\theta_0 = 0$.

The corresponding moment for x in that case would be

$$\langle x^n(t)|\theta_0\rangle_r = \mathrm{e}^{-rt}\langle x^n(t)|\theta_0\rangle_0 + r\int_0^t \mathrm{d}\tau \mathrm{e}^{-r\tau}\int \mathrm{d}\theta' P_0(\theta', t-\tau|\theta_0)\langle x^n(\tau)|\theta'\rangle. \tag{45}$$

Next, we calculate the second moment of x for the anisotropic particle using equation (8) and $n = 2$ in equation (45), resulting in

$$\begin{aligned}\langle x^2(t)|\theta_0\rangle_r &= \mathrm{e}^{-rt}2k_BT\left[\bar{\Gamma}t + \frac{\Delta\Gamma}{2}\cos 2\theta_0\left(\frac{1-\mathrm{e}^{-4D_\theta t}}{4D_\theta}\right)\right] \\ &+ r\int_0^t \mathrm{d}\tau \mathrm{e}^{-r\tau}\int \mathrm{d}\theta' \frac{\mathrm{e}^{-\frac{(\theta'-\theta_0)^2}{4D_\theta(t-\tau)}}}{\sqrt{4\pi D_\theta(t-\tau)}}2k_BT \\ &\times\left[\bar{\Gamma}\tau + \frac{\Delta\Gamma}{2}\cos 2\theta'\left(\frac{1-\mathrm{e}^{-4D_\theta\tau}}{4D_\theta}\right)\right] \\ &= \frac{2k_BT\bar{\Gamma}}{r} - \left(\frac{2k_BT\bar{\Gamma}}{r} - \frac{k_BT\Delta\Gamma\cos 2\theta_0}{4D_\theta - r}\right)\mathrm{e}^{-rt} \\ &- \frac{k_BT\Delta\Gamma\cos 2\theta_0}{4D_\theta - r}\mathrm{e}^{-4D_\theta t}.\end{aligned} \tag{46}$$

Similarly, one can also calculate $\langle y^2(t)|\theta_0\rangle_r$ and the cross-correlation $\langle x(t)y(t)|\theta_0\rangle_r$ in the presence of resetting. We find

$$\langle y^2(t)|\theta_0\rangle_r = \frac{2k_BT\bar{\Gamma}}{r} - \left(\frac{2k_BT\bar{\Gamma}}{r} + \frac{k_BT\Delta\Gamma\cos 2\theta_0}{4D_\theta - r}\right)\mathrm{e}^{-rt} + \frac{k_BT\Delta\Gamma\cos 2\theta_0}{4D_\theta - r}\mathrm{e}^{-4D_\theta t} \tag{47}$$

$$\langle x(t)y(t)|\theta_0\rangle_r = \frac{2k_BT\Delta\Gamma\sin 2\theta_0}{2(4D_\theta - r)}\left(\mathrm{e}^{-rt} - \mathrm{e}^{-4D_\theta t}\right). \tag{48}$$

Note that in the limit $r \to 4D_\theta$, the above equations remain well-defined if the limit is taken carefully. In the long time limit, both $\langle x^2(t)|\theta_0\rangle_r$ and $\langle y^2(t)|\theta_0\rangle_r$ approach $\frac{2k_BT\bar{\Gamma}}{r}$, and the steady state ratio of the variances, K_r becomes 1. The cross-correlation $\langle x(t)y(t)|\theta_0\rangle_r$ will be zero in the long time limit, but at intermediate times, $\langle x(t)y(t)|\theta_0\rangle_r$ shows a non-monotonic behavior against time. The initial growth is similar to what is seen in the absence of resetting, while resets exponentially decrease the correlations at later times. Therefore, as the state at late time has no cross-correlations and no anisotropy, the steady-state distribution for x will become $P_r(x) =$

$\frac{\alpha(r)}{2}\exp(-\alpha(r)|x|)$, with $\alpha(r)=\sqrt{r/\bar{D}}$, which is independent of D_θ. Due to isotropy at late time, the distribution in the y direction will be identical.

5. Orientational resetting

Finally, we consider the case of orientational resetting, where θ undergoes resets while the x and y variables do not undergo resets. Again, we follow the general discussion in section 2.2, leading to the last renewal equation

$$\begin{aligned}P_r(x,y,\theta,t|0,0,\theta_0) &= \mathrm{e}^{-rt}P_0(x,y,\theta,t|0,0,\theta_0)\\ &+ r\int_0^t \mathrm{d}\tau \mathrm{e}^{-r\tau}\int \mathrm{d}x'\int \mathrm{d}y'\\ &\times \int \mathrm{d}\theta' P_r(x',y',\theta',t-\tau|0,0,\theta_0)\\ &\times P_0(x,y,\theta,\tau|x',y',\theta_0). \end{aligned} \tag{49}$$

At the time of the last resetting $t-\tau$, the system is in some arbitrary state (x',y',θ'). As only θ is reset to θ_0, the system proceeds to evolve towards (x,y,θ) from the new initial condition (x',y',θ_0). The propagator for x for this case can be obtained by integrating the above equation over y, $y'\,\theta$, and θ',

$$\begin{aligned}P_r(x,t|0,\theta_0) &= \mathrm{e}^{-rt}P_0(x,t|0,\theta_0)\\ &+ r\int_0^t \mathrm{d}\tau \mathrm{e}^{-r\tau}\int \mathrm{d}x' P_r(x',t-\tau|0,\theta_0)\\ &\times P_0(x,\tau|x',\theta_0). \end{aligned} \tag{50}$$

In the case of complete and translational resetting, the renewal equations for the spatial moments could be expressed explicitly in terms of the corresponding densities without resetting. However, in the present case the probability density $P_r(x,t|0,\theta_0)$ is not given explicitly, as it appears both on the left-hand-side and inside the integral on the right-hand-side of the renewal equation.

In order to calculate the late-time moments, one can decouple the equation through the use of Fourier transforms in space and a Laplace transform in time under the assumption of spatial homogeneity. Recently, [73] studied the late-time behavior of the moments for this class of problems, where it was shown that the effective diffusion coefficients take the form

$$D_{\mathrm{eff}}^{(x)} = \lim_{t\to\infty}\frac{\langle x^2(t)\rangle_r}{2t} = \frac{r^2}{2}\mathcal{L}_r\left[\langle x^2(t)|\theta_0\rangle_0\right] \tag{51}$$

$$D_{\mathrm{eff}}^{(y)} = \lim_{t\to\infty}\frac{\langle y^2(t)\rangle_r}{2t} = \frac{r^2}{2}\mathcal{L}_r\left[\langle y^2(t)|\theta_0\rangle_0\right] \tag{52}$$

where $\mathcal{L}_r$ denotes a Laplace transform evaluated at r. Using the mean squared displacement for the problem without resetting, we immediately arrive at

$$D_{\mathrm{eff}}^{(x)} = k_BT\left(\bar{\Gamma}+\frac{r\Delta\Gamma\cos 2\theta_0}{2(r+4D_\theta)}\right) \tag{53}$$

$$D_{\mathrm{eff}}^{(y)} = k_BT\left(\bar{\Gamma}-\frac{r\Delta\Gamma\cos 2\theta_0}{2(r+4D_\theta)}\right). \tag{54}$$

In order to obtain a full time-dependent solution of the moments, we make use of the fact that the positions are themselves not coupled, but determined solely by the orientation θ. Hence, the mean squared displacement takes the same mathematical form as in the case of no resetting, equation (8), but now with the orientational dynamics subject to resets:

$$\langle x^2(t)|\theta_0\rangle_r = 2k_BT\int_0^t \mathrm{d}t'\left[\bar{\Gamma}+\frac{\Delta\Gamma}{2}\langle\cos\theta(t')|\theta_0\rangle_r\right]. \tag{55}$$

To calculate $\langle\cos\theta(t')|\theta_0\rangle_r$ in the presence of resetting, we use the last renewal equation only for θ, which takes the simple form

$$P_r(\theta,t|\theta_0) = \mathrm{e}^{-rt}P_0(\theta,t|\theta_0) + r\int_0^t \mathrm{d}\tau \mathrm{e}^{-r\tau}P_0(\theta,\tau|\theta_0). \tag{56}$$

Multiplying with $\cos 2\theta$ and integrating results in

$$\begin{aligned}\langle\cos 2\theta(t)|\theta_0\rangle_r &= \mathrm{e}^{-rt}\langle\cos 2\theta(t)|\theta_0\rangle_0\\ &+ r\int_0^t \mathrm{d}\tau \mathrm{e}^{-r\tau}\langle\cos 2\theta(\tau)|\theta_0\rangle_0\\ &= \cos(2\theta_0)\mathrm{e}^{-(r+4D_\theta)t}\\ &+ \frac{r\cos 2\theta_0}{r+4D_\theta}\left(1-\mathrm{e}^{-(r+4D_\theta)t}\right) \end{aligned} \tag{57}$$

Using equation (55), we find

$$\begin{aligned}\langle x^2(t)|\theta_0\rangle_r &= 2k_BT\int_0^t \mathrm{d}t'\left[\bar{\Gamma}+\frac{\Delta\Gamma}{2}\langle\cos\theta(t')|\theta_0\rangle_r\right]\\ &= 2k_BT\left[\left(\bar{\Gamma}+\frac{r\Delta\Gamma\cos 2\theta_0}{2(r+4D_\theta)}\right)t + \frac{2D_\theta\Delta\Gamma\cos 2\theta_0}{(r+4D_\theta)^2}\right.\\ &\left.\times\left(1-\mathrm{e}^{-(r+4D_\theta)t}\right)\right] \end{aligned} \tag{58}$$

Similarly, one can also calculate $\langle y^2(t)|\theta_0\rangle_r$ and the cross-correlation $\langle x(t)y(t)|\theta_0\rangle_r$ in the presence of resetting, resulting in

$$\begin{aligned}\langle y^2(t)|\theta_0\rangle_r &= 2k_BT\left[\left(\bar{\Gamma}-\frac{r\Delta\Gamma\cos 2\theta_0}{2(r+4D_\theta)}\right)t - \frac{2D_\theta\Delta\Gamma\cos 2\theta_0}{(r+4D_\theta)^2}\right.\\ &\left.\times\left(1-\mathrm{e}^{-(r+4D_\theta)t}\right)\right] \end{aligned} \tag{59}$$

$$\begin{aligned}\langle x(t)y(t)|\theta_0\rangle_r &= 2k_BT\int_0^t \mathrm{d}t'\left[\frac{\Delta\Gamma}{2}\langle\sin\theta(t')|\theta_0\rangle_r\right]\\ &= 2k_BT\left[\frac{r\Delta\Gamma\sin 2\theta_0}{2(r+4D_\theta)}t + \frac{2D_\theta\Delta\Gamma\sin 2\theta_0}{(r+4D_\theta)^2}\right.\\ &\left.\times\left(1-\mathrm{e}^{-(r+4D_\theta)t}\right)\right]. \end{aligned} \tag{60}$$

In the long time limit, since all expressions grow linearly in time, we can neglect the constant offset in the above equations,

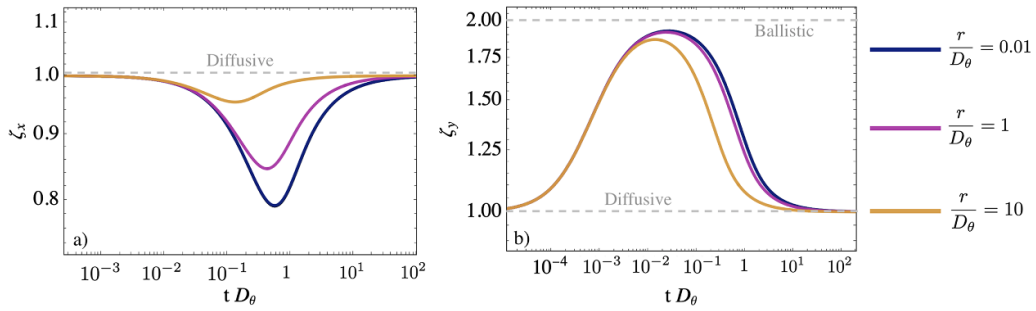

Figure 6. Dynamical exponents $\zeta_x(t)$ and $\zeta_y(t)$ for the mean squared displacement in the x and y direction for various values of resetting rate, in the case of orientational resets. The black line shows the exponents without resetting. Parameters are set to $\bar{\Gamma} = 1.0$, $\Delta\Gamma = 0.001$, with initial orientation $\theta_0 = 0$.

and the variances of the particle's position in the xy plane and the cross-correlations between x and y can be written as

$$\langle x^2(t)\,|\theta_0\rangle_r \approx 2k_BT\left(\bar{\Gamma} + \frac{r\Delta\Gamma\cos 2\theta_0}{2(r+4D_\theta)}\right)t \tag{61}$$

$$\langle y^2(t)\,|\theta_0\rangle_r \approx 2k_BT\left(\bar{\Gamma} - \frac{r\Delta\Gamma\cos 2\theta_0}{2(r+4D_\theta)}\right)t \tag{62}$$

which agrees with the predictions made in equations (53) and (54). The transient behavior can once again be understood by considering the dynamical exponents of the motion in the x and y directions. Figure (6) shows these exponents for the case $\theta_0 = 0$. In this case, the motion in the x direction undergoes a subdiffusive regime before re-entering a diffusing regime at late times. The dynamics in the y direction conversely goes through superdiffusive regime, before also re-entering a diffusive regime.

In contrast to the other resetting schemes considered so far, we now also have a cross correlation that at late times grows as

$$\langle x(t)\,y(t)\,|\theta_0\rangle_r \approx 2k_BT\frac{r\Delta\Gamma\sin 2\theta_0}{2(r+4D_\theta)}t. \tag{63}$$

Linear growth of the cross correlations has also been seen, for example, in multithermostat Brownian systems under the effect of a Lorentz force [77].

The steady state ratio of the variances, K_r, in the presence of resetting is given as

$$K_r = \frac{\langle x^2(t)\,|\theta_0\rangle_r}{\langle y^2(t)\,|\theta_0\rangle_r} = \frac{\left(\bar{\Gamma} + \frac{r\Delta\Gamma\cos 2\theta_0}{2(r+4D_\theta)}\right)}{\left(\bar{\Gamma} - \frac{r\Delta\Gamma\cos 2\theta_0}{2(r+4D_\theta)}\right)} \tag{64}$$

Using $\bar{D} = k_BT\bar{\Gamma}$, we see that this is exactly the degree of anisotropy as in the case of complete resetting. While the degree of anisotropy is the same, the dynamics is different. In particular, we obtain a non-zero cross-correlation between x and y which also grows linearly with time, while for complete resetting the same cross correlations saturates.

In the long time limit, we can expect that the two-dimensional probability distribution in the Cartesian components will be Gaussian due to the central limit theorem, given as

$$P(x,y,t) = \frac{1}{4\pi t\sqrt{\mathrm{Det}\,(\mathbb{D}_{\mathrm{eff}})}}\exp\left[-\frac{1}{4t}(x,y)^{\mathrm{T}}\,\mathbb{D}_{\mathrm{eff}}^{-1}(x,y)\right], \tag{65}$$

where the effective diffusion tensor is given as

$$\mathbb{D}_{\mathrm{eff}} = 2k_BT\begin{bmatrix} \bar{\Gamma} + \frac{r\Delta\Gamma\cos 2\theta_0}{2(r+4D_\theta)} & \frac{r\Delta\Gamma\sin 2\theta_0}{2(r+4D_\theta)} \\ \frac{r\Delta\Gamma\sin 2\theta_0}{2(r+4D_\theta)} & \bar{\Gamma} - \frac{r\Delta\Gamma\cos 2\theta_0}{2(r+4D_\theta)} \end{bmatrix}. \tag{66}$$

The marginal probability distribution for x can be obtained by integrating the y variable, given as

$$P(x,t) = \int \mathrm{d}y P(x,y,t) = \frac{1}{\sqrt{4\pi D_{\mathrm{eff}}^{(x)}t}}\exp\left[-\frac{x^2}{4D_{\mathrm{eff}}^{(x)}t}\right]. \tag{67}$$

The same argument holds for the marginal probability distribution for y. However, the long-time probability distribution in equation (65) cannot be separated into a product of two independent distributions in the x and y directions. Figure (7) shows the density plots of the steady state probability distribution of the position of the particle. The steady state probability distribution is isotropic without resetting, and the degree of anisotropy grows along the direction of initial angle θ_0 (dashed line in figure (7)).

It is worth considering a somewhat more intuitive approach to understand the unboundedness of the cross-correlation between x and y with time. We consider the correlation coefficient defined as $C(t) = \frac{\langle x(t)y(t)|\theta_0\rangle}{\sqrt{\langle x^2(t)|\theta_0\rangle}\sqrt{\langle y^2(t)|\theta_0\rangle}}$. In the presence of only orientational resetting, $C(t)$ will become constant in the long-time limit, as can be readily verified by using the above results. This is similar to the case of the resetting all the variable, where $C(t)$ will also be a constant, which is an immediate consequence of the fact that a steady state is reached in this case. This non-zero correlation between the two spatial directions results from the presence of orientational resetting, while for translational resetting, $C(t)$ will be zero in the long-time limit.

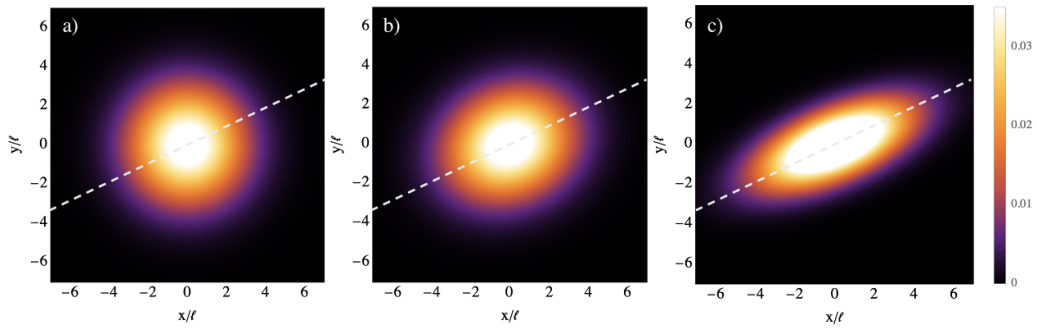

Figure 7. Fixed-time ($tD_\theta = 4$) two-dimensional positional densities under orientational resetting at different rates: $r = 0$ (panel (a)), $r = 2D_\theta$ (panel (b)) and $r = 5D_\theta$ (panel (c)). Lengthscale is set by $\ell^2 = 2k_BT\bar{\Gamma}/D_\theta$. The dashed line shows initial angle θ_0. Parameters are set to $\theta_0 = \pi/8, D_\theta = 1.\Gamma_{||} = 1, \Gamma_\perp = 0.001$.

6. Discussion

In this article, we have explored the effects of shape asymmetry on the two-dimensional diffusive motion of an anisotropic particle in the presence of stochastic resetting. In particular, we studied the short- and long-time behavior of moments, cross-correlations and steady-state distributions under various resetting protocols. It is well known that anisotropic diffusion persists only for very short times, and that isotropic diffusion is recovered at long-times. Hence, for practical purposes the short-time behavior can often be neglected and the movement of an asymmetric particle can be described by the Langevin equations for a point particle with an isotropic translational diffusion coefficient given by the average of the diffusion coefficients along the major and minor axes of the particle. This has been shown to be the case for example for a free particle and in a presence of a harmonic confinement in two dimensions [25].

We have shown that these assumptions are generally not valid for resetting schemes that include orientational resets, and can be restored only if we apply resetting of the translational degrees of freedom. In this case, the steady-state distribution, moments and cross-correlations are exactly equal to the case of a spherical particle in the presence of stochastic resetting. On the other hand, when orientational resetting takes place, the short-time anisotropy of the motion is promoted to late times. Both the case of complete resetting and orientational resetting display this, with the degree of anisotropy K_r being the same in the two cases. For complete resetting, we calculated both time-dependent moments and a perturbative steady state. For orientational resetting, we calculated the effective (anisotropic) diffusion tensor, which determines the effective Gaussian behavior at late times.

In future works, it would be interesting to study the first passage problem for an anisotropic diffusive particle in a two-dimensions in the presence of resetting. It would also be interesting to study resetting of other asymmetric particles, or to study the dynamics of resetting colloids in the presence of interactions. Intriguing effects of resetting could also be explored in three dimensions, both for rod-like particle with one orientational degree of freedom and for full anisotropic particles [78]. Recently, physical (finite-time) implementations of resetting through sharp intermittent confining potentials has been studied in the context of spherical Brownian particles, whereby the system can be described by a Langevin equation also in the resetting phase [53, 61, 64, 79–82]. Extending these findings to account for anisotropic particles, where also finite-time schemes for the orientation must be considered, presents an intriguing direction for further investigation.

Data availability statement

No new data were created or analysed in this study.

Acknowledgment

SC acknowledges support from the Alexander Von Humboldt foundation. KSO and HL acknowledge support by the Deutsche Forschungsgemeinschaft (DFG) within the Project LO 418/29-1.

Appendix. Derivation of last renewal equation from the Fokker-Planck approach

For the sake of completeness, we here briefly review the basic equations governing resetting processes when multiple degrees of freedom are involved, including both Fokker–Planck and renewal equations. As a simple example that can be generalized, we consider a system with two degrees of freedom x, y. We further assume that x is coupled to y, while the converse is not the case. This is similar to how the spatial variables in the anisotropic diffusion problem are both coupled to the angular variable, but not vice versa.

At constant rate r the system resets the variable x to x_0. This means that during a small time window dt the probability of resetting is rdt. Hence, conservation of probability can be

expressed as

$$P_r(x,y,t+\mathrm{d}t) = (1-r\mathrm{d}t)\left\langle P_r(x-\Delta_x, y-\Delta_y, t)\right\rangle_{\Delta_x,\Delta_y} + r\mathrm{d}t\delta(x-x_0)P_r(y,t). \tag{A1}$$

This expression accounts for all probability currents flowing into (x,y) during a small time step $\mathrm{d}t$. The first term corresponds to the cases without resetting, where the dynamics evolves into (x,y) by taking small random steps $\Delta_{x,y}$. The second term represents the resetting cases, where the delta function ensures that the only value of x that receives a contribution from resets is $x = x_0$. Furthermore, $P_r(y,t)$ is the marginal probability density of y, and makes sure that the y dynamics remains unchanged during the reset. The first term is the standard term in stochastic differential equations which turns into the Fokker–Planck operator $\hat{L}(x,y)$ when expanded in $\Delta_{x,y}$ and dt. The augmented Fokker–Planck equation with the resetting terms will in the continuum limit take the form

$$\begin{aligned}\frac{\partial P_r(x,y,t|x_0,y_0)}{\partial t} &= LP_r(x,y,t|x_0,y_0) - rP_r(x,y,t|x_0,y_0) \\ &\quad + r\delta(x-x_0)\int \mathrm{d}x' P_r(x',y,t|x_0,y_0) \\ &= LP_r(x,y,t|x_0,y_0) - rP_r(x,y,t|x_0,y_0) \\ &\quad + r\delta(x-x_0)P_r(y,t|x_0,y_0)\end{aligned} \tag{A2}$$

where L is the Fokker–Planck operator for the anisotropic particle given in equation (27) and we define $P_r(y,t|x_0,y_0) \equiv \int \mathrm{d}x' P_r(x',y,t|x_0,y_0)$. Taking the Fourier transform of equation (A2), one obtains

$$\begin{aligned}\frac{\partial \tilde{P}_r(k_1,k_2,t)}{\partial t} &= \tilde{L}\tilde{P}_r(k_1,k_2,t) - r\tilde{P}_r(k_1,k_2,t) \\ &\quad + r\tilde{P}_r(k_2,t|x_0,y_0)\mathrm{e}^{-ik_1x_0}\end{aligned} \tag{A3}$$

equation (A3) is rewritten as

$$\frac{\partial \tilde{P}_r(k_1,k_2,t)}{\partial t} + \left(-\tilde{L}+r\right)\tilde{P}_r(k_1,k_2,t) = r\tilde{P}_r(k_2,t|x_0,y_0)\mathrm{e}^{-ik_1x_0} \tag{A4}$$

Multiplying both sides of equation (A4) by the integrating factor $\mathrm{e}^{\left(-\tilde{L}+r\right)t}$, we get

$$\begin{aligned}&\mathrm{e}^{\left(-\tilde{L}+r\right)t}\frac{\partial \tilde{P}_r(k_1,k_2,t)}{\partial t} + \mathrm{e}^{\left(-\tilde{L}+r\right)t}\left(-\tilde{L}+r\right)\tilde{P}_r(k_1,k_2,t) \\ &= r\mathrm{e}^{\left(-\tilde{L}+r\right)t}\tilde{P}_r(k_2,t|x_0,y_0)\mathrm{e}^{-ik_1x_0}\end{aligned} \tag{A5}$$

which implies the differential equation

$$\frac{\partial}{\partial t}\left[\mathrm{e}^{\left(-\tilde{L}+r\right)t}\tilde{P}_r(k_1,k_2,t)\right] = r\mathrm{e}^{\left(-\tilde{L}+r\right)t}\tilde{P}_r(k_2,t|x_0,y_0)\mathrm{e}^{-ik_1x_0}. \tag{A6}$$

Integrating the above equation (A6), one can obtain

$$\begin{aligned}&\tilde{P}_r(k_1,k_2,t) - \mathrm{e}^{\left(\tilde{L}-r\right)t}\tilde{P}_r(k_1,k_2,0) \\ &= r\int_0^t \mathrm{d}t'\mathrm{e}^{\left(\tilde{L}-r\right)\left(t-t'\right)}\mathrm{e}^{-ik_1x_0}\tilde{P}_r(k_2,t|x_0,y_0).\end{aligned} \tag{A7}$$

Using the initial condition $P_r(x,y,0|x_0,y_0) = \delta(x-x_0)\delta(y-y_0)$, we obtain

$$\begin{aligned}&\tilde{P}_r(k_1,k_2,t|x_0,y_0) - \mathrm{e}^{-rt}\tilde{P}_0(k_1,k_2,t|x_0,y_0) \\ &= r\int_0^t \mathrm{d}t'\mathrm{e}^{-r\left(t-t'\right)}\tilde{P}_0(k_1,k_2,t-t'|x_0,0)\tilde{P}_r(k_2,t'|x_0,y_0).\end{aligned} \tag{A8}$$

After performing the inverse Fourier transformation of the above equation (A8), we have

$$\begin{aligned}P_r(x,y,t|x_0,y_0) &= \mathrm{e}^{-rt}P_0(x,y,t|x_0,y_0) \\ &\quad + r\int_0^t \mathrm{d}t'\int \mathrm{d}y'\mathrm{e}^{-r\left(t-t'\right)}P_0(x,y-y',t-t'|x_0,0) \\ &\quad \times P_r(y',t'|x_0,y_0).\end{aligned} \tag{A9}$$

For spatially homogeneous systems, the probability distribution satisfies

$$P_0(x-x',y-y',t) = P_0(x,y,t|x',y') \tag{A10}$$

resulting in

$$\begin{aligned}P_r(x,y,t|x_0,y_0) &= \mathrm{e}^{-rt}P_0(x,y,t|x_0,y_0) \\ &\quad + r\int_0^t \mathrm{d}t'\int \mathrm{d}y'\mathrm{d}x'\mathrm{e}^{-r\left(t-t'\right)}P_0(x,y,t-t'|x_0,y') \\ &\quad \times P_r(x',y',t'|x_0,y_0)\end{aligned} \tag{A11}$$

where we substituted the expression for $P_r(y,t|x_0,y_0)$. Letting $\tau \equiv t-t'$, we arrive at

$$\begin{aligned}P_r(x,y,t|x_0,y_0) &= \mathrm{e}^{-rt}P_0(x,y,t|x_0,y_0) \\ &\quad + r\int_0^t \mathrm{d}\tau\mathrm{e}^{-r\tau}\int \mathrm{d}y'\mathrm{d}x' \\ &\quad \times P_r(x',y',t-\tau|x_0,y_0)P_0(x,y,\tau|x_0,y').\end{aligned} \tag{A12}$$

This is the last renewal equation, which has the natural interpretation as a decomposition into trajectories going from (x_0,y_0) to an intermediate random state at the time of the last reset, (x',y'), before the system resets to (x_0,y') and evolves to the final state (x,y).

ORCID iDs

Subhasish Chaki https://orcid.org/0000-0002-0740-4433
Kristian Stølevik Olsen https://orcid.org/0000-0002-9982-6413

References

[1] Bawden F, Pirie N, Bernal J and Fankuchen I 1936 Liquid crystalline substances from virus-infected plants *Nature* **138** 1051
[2] Wen X, Meyer R B and Caspar D 1989 Observation of smectic-A ordering in a solution of rigid-rod-like particles *Phys. Rev. Lett.* **63** 2760
[3] Graf H and Löwen H 1999 Phase diagram of tobacco mosaic virus solutions *Phys. Rev.* E **59** 1932

[4] Doostmohammadi A, Thampi S P and Yeomans J M 2016 Defect-mediated morphologies in growing cell colonies *Phys. Rev. Lett.* **117** 048102

[5] Gray C G, Gubbins K E and Joslin C G 1984 *Theory of Molecular Fluids: Volume 2: Applications* (International Monographs on Ch)

[6] Narayan V, Ramaswamy S and Menon N 2007 Long-lived giant number fluctuations in a swarming granular nematic *Science* **317** 105

[7] Ivlev A, Morfill G, Lowen H and Royall C P 2012 *Complex plasmas and colloidal dispersions: particle-resolved studies of classical liquids and solids* vol 5 (World Scientific Publishing Company)

[8] Löwen H 1994 Brownian dynamics of hard spherocylinders *Phys. Rev.* E **50** 1232

[9] Bolhuis P and Frenkel D 1997 Tracing the phase boundaries of hard spherocylinders *J. Chem. Phys.* **106** 666

[10] Dijkstra M 2014 Entropy-driven phase transitions in colloids: from spheres to anisotropic particles *Adv. Chem. Phys.* **156** 35

[11] Löwen H 1999 Anisotropic self-diffusion in colloidal nematic phases *Phys. Rev.* E **59** 1989

[12] Roller J, Laganapan A, Meijer J-M, Fuchs M and Zumbusch A 2021 Observation of liquid glass in suspensions of ellipsoidal colloids *Proc. Natl Acad. Sci. USA* **118** e2018072118

[13] Wu N, Lee D and Striolo A 2018 *Anisotropic Particle Assemblies: Synthesis, Assembly, Modeling and Applications* (Elsevier)

[14] Glotzer S C and Solomon M J 2007 Anisotropy of building blocks and their assembly into complex structures *Nat. Mater.* **6** 557

[15] Sacanna S and Pine D J 2011 Shape-anisotropic colloids: building blocks for complex assemblies *Curr. Opin. Colloid Interface Sci.* **16** 96

[16] Thorkelsson K, Bai P and Xu T 2015 Self-assembly and applications of anisotropic nanomaterials: a review *Nano Today* **10** 48

[17] Simeonidis K, Morales M P, Marciello M, Angelakeris M, de La Presa P, Lazaro-Carrillo A, Tabero A, Villanueva A, Chubykalo-Fesenko O and Serantes D 2016 *In-situ* particles reorientation during magnetic hyperthermia application: shape matters twice *Sci. Rep.* **6** 38382

[18] Perrin F 1934 Mouvement brownien d'un ellipsoide-I. Dispersion diélectrique pour des molécules ellipsoidales *J. Phys. Radium* **5** 497

[19] Perrin F 1936 Mouvement brownien d'un ellipsoide (II). Rotation libre et dépolarisation des fluorescences. Translation et diffusion de molécules ellipsoidales *J. Phys. Radium* **7** 1

[20] Koenig S H 1975 Brownian motion of an ellipsoid. a correction to perrin's results *Biopolymers* **14** 2421

[21] Han Y, Alsayed A M, Nobili M, Zhang J, Lubensky T C and Yodh A G 2006 Brownian motion of an ellipsoid *Science* **314** 626

[22] Bicout D J and Field M J 1996 Stochastic dynamics simulations of macromolecular diffusion in a model of the cytoplasm of escherichia coli *J. Phys. Chem.* B **100** 2489

[23] Schnell S and Turner T 2004 Reaction kinetics in intracellular environments with macromolecular crowding: simulations and rate laws *Prog. Biophys. Mol. Biol.* **85** 235

[24] Han Y, Alsayed A, Nobili M and Yodh A G 2009 Quasi-two-dimensional diffusion of single ellipsoids: aspect ratio and confinement effects *Phys. Rev.* E **80** 011403

[25] Grima R and Yaliraki S 2007 Brownian motion of an asymmetrical particle in a potential field *J. Chem. Phys.* **127** 084511

[26] Levernier N, Bénichou O and Voituriez R 2016 Mean first-passage time of an anisotropic diffusive searcher *J. Phys. A: Math. Theor.* **50** 024001

[27] Ghosh A, Mandal S and Chakraborty D 2022 Persistence of an active asymmetric rigid Brownian particle in two dimensions *J. Chem. Phys.* **157** 194905

[28] Ghosh A and Chakraborty D 2020 Persistence in Brownian motion of an ellipsoidal particle in two dimensions *J. Chem. Phys.* **152** 174901

[29] Anchutkin G, Holubec V and Cichos F 2024 Run-and-tumble motion of ellipsoidal swimmers (arXiv:2402.04697)

[30] Shemi O and Solomon M J 2018 Self-propulsion and active motion of Janus ellipsoids *J. Phys. Chem.* B **122** 10247

[31] Marino R, Eichhorn R and Aurell E 2016 Entropy production of a Brownian ellipsoid in the overdamped limit *Phys. Rev.* E **93** 012132

[32] Evans M R and Majumdar S N 2011 Diffusion with stochastic resetting *Phys. Rev. Lett.* **106** 160601

[33] Evans M R and Majumdar S N 2011 Diffusion with optimal resetting *J. Phys. A: Math. Theor.* **44** 435001

[34] Evans M R, Majumdar S N and Schehr G 2020 Stochastic resetting and applications *J. Phys. A: Math. Theor.* **53** 193001

[35] Majumdar S N, Sabhapandit S and Schehr G 2015 Dynamical transition in the temporal relaxation of stochastic processes under resetting *Phys. Rev.* E **91** 052131

[36] Gupta D 2019 Stochastic resetting in underdamped Brownian motion *J. Stat. Mech.* **2019** 033212

[37] Pal A 2015 Diffusion in a potential landscape with stochastic resetting *Phys. Rev.* E **91** 012113

[38] Nagar A and Gupta S 2016 Diffusion with stochastic resetting at power-law times *Phys. Rev.* E **93** 060102

[39] Reuveni S 2016 Optimal stochastic restart renders fluctuations in first passage times universal *Phys. Rev. Lett.* **116** 170601

[40] Besga B, Bovon A, Petrosyan A, Majumdar S N and Ciliberto S 2020 Optimal mean first-passage time for a Brownian searcher subjected to resetting: experimental and theoretical results *Phys. Rev. Res.* **2** 032029

[41] Faisant F, Besga B, Petrosyan A, Ciliberto S and Majumdar S N 2021 Optimal mean first-passage time of a Brownian searcher with resetting in one and two dimensions: experiments, theory and numerical tests *J. Stat. Mech. Theory Exp.* **2021** 113203

[42] Pal A, Kuśmierz Ł and Reuveni S 2020 Search with home returns provides advantage under high uncertainty *Phys. Rev. Res.* **2** 043174

[43] Durang X, Lee S, Lizana L and Jeon J-H 2019 First-passage statistics under stochastic resetting in bounded domains *J. Phys. A: Math. Theor.* **52** 224001

[44] Tucci G, Gambassi A, Majumdar S N and Schehr G 2022 First-passage time of run-and-tumble particles with noninstantaneous resetting *Phys. Rev.* E **106** 044127

[45] Tal-Friedman O, Pal A, Sekhon A, Reuveni S and Roichman Y 2020 Experimental realization of diffusion with stochastic resetting *J. Phys. Chem. Lett.* **11** 7350

[46] Toledo-Marin J Q and Boyer D 2022 First passage time and information of a one-dimensional Brownian particle with stochastic resetting to random positions (arXiv:2206.14387)

[47] Ahmad S, Rijal K and Das D 2022 First passage in the presence of stochastic resetting and a potential barrier (arXiv:2202.03766)

[48] Ahmad S, Nayak I, Bansal A, Nandi A and Das D 2019 First passage of a particle in a potential under stochastic resetting: A vanishing transition of optimal resetting rate *Phys. Rev.* E **99** 022130

[49] Xu P, Zhou T, Metzler R and Deng W 2022 Stochastic harmonic trapping of a lévy walk: transport and first-passage dynamics under soft resetting strategies *New J. Phys.* **24** 033003
[50] Ray S 2020 Space-dependent diffusion with stochastic resetting: A first-passage study *J. Chem. Phys.* **153** 234904
[51] Pal A and Prasad V 2019 First passage under stochastic resetting in an interval *Phys. Rev.* E **99** 032123
[52] Pal A, Kostinski S and Reuveni S 2022 The inspection paradox in stochastic resetting *J. Phys. A: Math. Theor.* **55** 021001
[53] Mercado-Vásquez G, Boyer D and Majumdar S N 2022 Reducing mean first passage times with intermittent confining potentials: a realization of resetting processes *J. Stat. Mech.* **2022** 093202
[54] Bressloff P C 2020 Directed intermittent search with stochastic resetting *J. Phys. A: Math. Theor.* **53** 105001
[55] Bressloff P C 2020 Modeling active cellular transport as a directed search process with stochastic resetting and delays *J. Phys. A: Math. Theor.* **53** 355001
[56] Fuchs J, Goldt S and Seifert U 2016 Stochastic thermodynamics of resetting *Europhys. Lett.* **113** 60009
[57] Pal A and Rahav S 2017 Integral fluctuation theorems for stochastic resetting systems *Phys. Rev.* E **96** 062135
[58] Pal A, Reuveni S and Rahav S 2021 Thermodynamic uncertainty relation for systems with unidirectional transitions *Phys. Rev. Res.* **3** 013273
[59] Gupta D, Plata C A and Pal A 2020 Work fluctuations and Jarzynski equality in stochastic resetting *Phys. Rev. Lett.* **124** 110608
[60] Gupta D and Plata C A 2022 Work fluctuations for diffusion dynamics submitted to stochastic return *New J. Phys.* **24** 113034
[61] Mori F, Olsen K S and Krishnamurthy S 2023 Entropy production of resetting processes *Phys. Rev. Res.* **5** 023103
[62] Olsen K S, Gupta D, Mori F and Krishnamurthy S 2023 Thermodynamic cost of finite-time stochastic resetting (arXiv:2310.11267)[cond-mat.stat-mech]
[63] Pal P S, Pal A, Park H and Lee J S 2023 Thermodynamic trade-off relation for first passage time in resetting process misc (arXiv:2305.04562)
[64] Olsen K S and Gupta D 2024 Thermodynamic work of partial resetting *J. Phys. A: Math. Theor.* **57** 245001
[65] Goerlich R, Li M, Pires L B, Hervieux P A, Manfredi G and Genet C 2023 Experimental test of landauer's principle for stochastic resetting (arXiv:2306.09503)
[66] Kumar V, Sadekar O and Basu U 2020 Active Brownian motion in two dimensions under stochastic resetting *Phys. Rev.* E **102** 052129
[67] Evans M R and Majumdar S N 2018 Run and tumble particle under resetting: a renewal approach *J. Phys. A: Math. Theor.* **51** 475003
[68] Santra I, Basu U and Sabhapandit S 2020 Run-and-tumble particles in two dimensions under stochastic resetting conditions *J. Stat. Mech.* **2020** 113206
[69] Baouche Y, Franosch T, Meiners M and Kurzthaler C 2024 Active Brownian particle under stochastic orientational resetting *New J. Phys.* **26** 073041
[70] Goswami K and Chakrabarti R 2021 Stochastic resetting and first arrival subjected to gaussian noise and Poisson white noise *Phys. Rev.* E **104** 034113
[71] Olsen K S 2023 Steady-state moments under resetting to a distribution *Phys. Rev.* E **108** 044120
[72] Abdoli I and Sharma A 2021 Stochastic resetting of active Brownian particles with Lorentz force *Soft Matter* **17** 1307
[73] Olsen K S and Löwen H 2024 Dynamics of inertial particles under velocity resetting *J. Stat. Mech.* **2024** 033210
[74] Besga B, Faisant F, Petrosyan A, Ciliberto S and Majumdar S N 2021 Dynamical phase transition in the first-passage probability of a Brownian motion *Phys. Rev.* E **104** L012102
[75] Tierno P 2014 Recent advances in anisotropic magnetic colloids: realization, assembly and applications *Phys. Chem. Chem. Phys.* **16** 23515
[76] Mayer D B, Sarmiento-Gómez E, Escobedo-Sánchez M A, Segovia-Gutiérrez J P, Kurzthaler C, Egelhaaf S U and Franosch T 2021 Two-dimensional Brownian motion of anisotropic dimers *Phys. Rev.* E **104** 014605
[77] Abdoli I, Kalz E, Vuijk H D, Wittmann R, Sommer J-U, Brader J M and Sharma A 2020 Correlations in multithermostat Brownian systems with Lorentz force *New J. Phys.* **22** 093057
[78] Wittkowski R and Löwen H 2012 Self-propelled Brownian spinning top: dynamics of a biaxial swimmer at low Reynolds numbers *Phys. Rev.* E **85** 021406
[79] Santra I, Das S and Nath S K 2021 Brownian motion under intermittent harmonic potentials *J. Phys. A: Math. Theor.* **54** 334001
[80] Mercado-Vásquez G, Boyer D, Majumdar S N and Schehr G 2020 Intermittent resetting potentials *J. Stat. Mech.* **2020** 113203
[81] Gupta D, Plata C A, Kundu A and Pal A 2020 Stochastic resetting with stochastic returns using external trap *J. Phys. A: Math. Theor.* **54** 025003
[82] Gupta D, Pal A and Kundu A 2021 Resetting with stochastic return through linear confining potential *J. Stat. Mech.* **2021** 043202